

Hyperinnervation of Mesenteric Arteries in Spontaneously Hypertensive Rats by Sympathetic but Not Primary Afferent Axons

An Ultrastructural Analysis

Susan E. Luff^a Simone B. Young^a Elspeth M. McLachlan^b

^aMonash Micro Imaging, School of Biomedical Science, Monash University, Clayton, and ^bPrince of Wales Medical Research Institute and University of New South Wales, Randwick, Australia

Key Words

Nerve growth factor · Neuromuscular junctions · Substance P · Vascular innervation

Abstract

Hypertrophy of the perivascular plexus is thought to play a role in the development of hypertension in spontaneously hypertensive rats (SHR). However, it is not known whether the sympathetic varicosities are more numerous or larger, or form more neurovascular junctions. Further, a parallel hypertrophy of primary afferent terminals around the vessels might modulate any effects of hypertrophied sympathetic terminals. We have investigated the perivascular plexus around second-order mesenteric arteries of SHR and Wistar-Kyoto (WKY) rats by electron microscopy. Noradrenergic terminals were identified by the presence of small granular vesicles after chromaffin fixation, and substance P (SP+) afferent axons were identified by immunohistochemistry. The numbers of noradrenergic axon and varicosity profiles were higher (48 and 25%, respectively) in SHR than in WKY

rats, and the majority lay closer to the medio-adventitial border. In contrast, there was no difference in the numbers of SP+ axons. Sympathetic and SP+ varicosities were indistinguishable in size, shape, vesicle content and mitochondrion content between each other and between the strains. However, both the number of neuromuscular junctions and the proportion of varicosities that formed them in SHR arteries were more than double those in WKY vessels. The data clearly show that hyperinnervation in SHR is specific for noradrenergic axons.

Copyright © 2005 S. Karger AG, Basel

Introduction

Hyperinnervation of the vasculature by sympathetic axons has been implicated in the development and maintenance of hypertension. The evidence is that (i) circulating noradrenaline (NA) levels are higher in borderline hypertensive patients [1], (ii) the NA content of blood vessels and the immunofluorescence of the catecholaminergic innervation around them are greater [2] and (iii) the volume of nervous tissue in the perivascular plexus is greater [3, 4] in spontaneously hypertensive rats (SHR). None of these studies indicate whether the hyperinnervation results from increased numbers of axons and/or var-

This work was supported by the National Heart Foundation of Australia and the National Health and Medical Research Council.

icosities or from enlargement of individual axons and their varicosities. Further, the ultrastructural studies [3] did not distinguish whether the greater neural volume involved only noradrenergic axons. This information can only be derived from ultrastructural studies when individual varicosities are identified histochemically, as has recently been done in Wistar-Kyoto (WKY) rats [5].

The perivascular plexus around the rat mesenteric artery contains, in addition to sympathetic axons, a population of terminals arising from primary afferent neurones with their cell bodies in the dorsal root ganglia. The great majority of these afferent neurones contain two neuropeptides, substance P (SP) and calcitonin-gene-related peptide (CGRP). Perivascular stimulation releases these peptides with CGRP acting as a potent vasodilator in this vessel [6, 7] whereas neurally released SP has no post-junctional effect [6]. Although it has been reported that exogenous SP inhibits the electrically evoked release of NA [8], application of capsaicin to deplete the neuropeptides did not modify the amplitude of either NA-oxidation currents or purinergic excitatory junction potentials evoked by perivascular stimulation [9]. Primary afferent neurones containing these peptides are, like sympathetic post-ganglionic neurones, dependent on tissue-derived neuronal growth factors, including nerve growth factor (NGF), both during development and for trophic maintenance in the adult animal [10, 11]. Only the noradrenergic varicosities form neurovascular junctions on the mesenteric artery [5].

Systemic treatment with anti-NGF blocks the initiation of hypertension in SHR [10, 12, 13], suggesting that enhanced expression of NGF or its receptors may be responsible for the noradrenergic hyperinnervation. With regard to the afferent innervation in SHR, it is possible that (i) afferent terminals are more abundant than in control (WKY) animals due to higher NGF levels in the vicinity of the artery, (ii) they are present at normal densities because the genetic mutation specifically affects sympathetic axons or (iii) fewer primary afferent axons are present because the available NGF is preferentially utilised by the hypertrophied sympathetic axons. In the present study, we sought to distinguish between these possibilities.

We have therefore undertaken a detailed quantitative ultrastructural analysis of the perivascular plexus of arteries from 7-week-old SHR and WKY rats. Second-order branches of mesenteric arteries have been examined after immunohistochemical treatment to demonstrate SP and after chromaffin fixation to enhance the electron density of the cores of small granular vesicles present in norad-

renergic varicosities. Immunoreactivity for SP rather than CGRP using the antibodies available to us provided less ambiguous material for the identification of immunopositive axons and terminals at the ultrastructural level. Single and serial sections have been analysed to determine the distribution, density and dimensions of axons and varicosities identified as SP positive (SP+) or noradrenergic. The data clearly indicate that the hyperinnervation in SHR is restricted to the sympathetic population of axons and that it involves the numbers rather than the size of the component varicosities. Furthermore, the number of sympathetic neurovascular junctions is more than twice that in control arteries.

Methods

Tissue Preparation for Electron Microscopy

Male Wistar rats of the Kyoto and SHR strains aged 50 days were fixed by perfusion with 4% paraformaldehyde/0.1% glutaraldehyde in 0.1 M phosphate buffer (pH 7.2) under deep anaesthesia (70 mg/kg pentobarbitone i.p.) using a nitrite prewash, as described previously [5]. The perfusion method ensured that the vasculature was fixed at maximum dilation and at a standardised flow rate for all animals (fig. 1). Second-order branches of the superior mesenteric artery from the ileum region of the small intestine were immediately dissected on ice in fresh fixative consisting of 4% paraformaldehyde plus 1% glutaraldehyde in 0.1 M cacodylate buffer (pH 7.4) for 2 h and post-fixed on 2% osmium tetroxide in 0.1 M sodium cacodylate buffer. This material was processed for standard electron microscopy and used for measurements of axon and varicosity densities.

Immunohistochemistry. To demonstrate SP, perfusion-fixed vessels were post-fixed for 18 h in 4% paraformaldehyde/1% glutaraldehyde in 0.1 M phosphate buffer (pH 7.2) at 4°C and then processed for immunohistochemical localisation of SP [5] prior to embedding in Epon. Short ribbons of 3–4 consecutive longitudinal sections (~100 nm thick and 900 µm long) were cut from vessels. The sections were placed on Formvar-coated single-slot grids. Three grids containing consecutive sections were prepared for each vessel. The middle grid of sections from immunostained vessels was stained with uranyl acetate and lead citrate; the other two grids were retained unstained. One stained section from the middle of the ribbon was used to determine the density of SP+ and SP negative (SP-) profiles (fig. 2a). Reference was made to the adjacent ribbons of unstained sections if the presence of immunoreactivity was ambiguous as the immunoreactivity was particularly clear in unstained sections [5]. Data from 6 WKY animals (2 vessels from each of 3 animals, 3 from each of 2 animals and 1 from 1 animal) and 5 SHR animals (2 from each of 4 animals and 3 from 1 animal) were analysed from material that had been immunostained for the presence of SP. Additional material from the two strains was processed in parallel for double-labelling fluorescence histochemistry to demonstrate the presence of vasoactive intestinal polypeptide (VIP), which has been reported to be present but sparse around rat mesenteric vessels [14]. Second-order arteries (1 cm long) from 7-week-old rats of both strains were fixed in Zamboni's fixative and

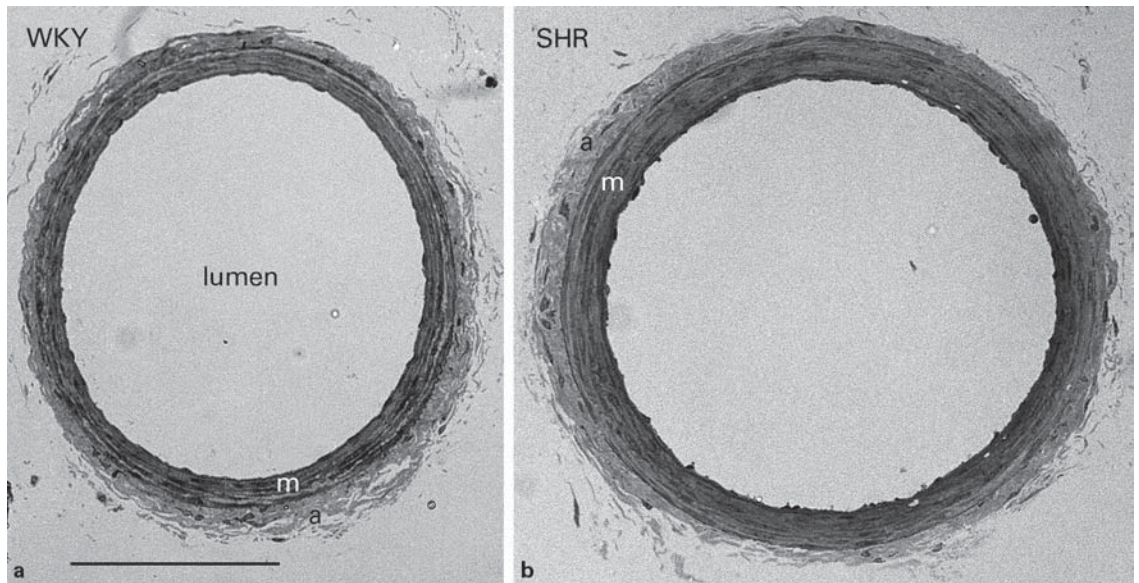


Fig. 1. Light micrographs of transverse sections of second-order branches of mesenteric arteries from WKY (**a**) and SHR (**b**) fixed in situ by perfusion under pressure. Calibration in **a** (bar = 100 μ m) applies to both micrographs. a = adventitia, m = media.

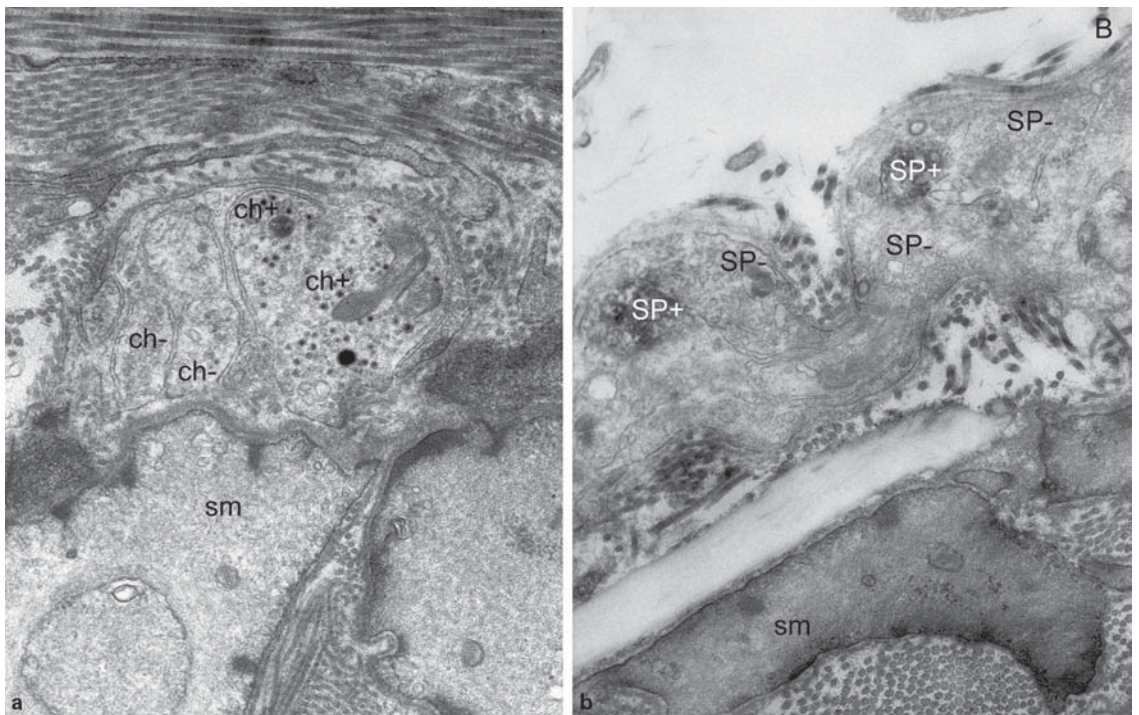


Fig. 2. Electron micrographs showing axon bundles around mesenteric arteries from SHR (**a**) and WKY rats (**b**). Distinct varicosities contain vesicles positive (ch+) or negative (ch-) for chromaffin (**a**) and immunoreactivity for SP (SP+ or SP-; **b**). sm = Arterial smooth muscle cells. Calibration in **b** (bar = 1 μ m) also applies to **a**.

processed as described previously [5]. Primary antibody to VIP raised in rabbit (Incstar, Stillwater, Minn., USA; 1:1,000) was applied overnight to 14- μm thick frozen longitudinal sections, together with antibody to tyrosine hydroxylase (TH) raised in mouse (Incstar, 1:500), followed by incubation in FITC-labelled anti-rabbit IgG (Amersham, Little Chalfont, UK) and CY3-labelled anti-mouse IgG (Jackson, Westgrove, Pa., USA). The location and density of VIP and TH axons was compared with that of SP and TH axons [5]. Control sections of rat and guinea pig ileum showed dense intramural plexuses of VIP-immunoreactive axons.

Identification of Catecholamine-Containing Axons. To identify catecholamine-containing axon terminals, vessels from the perfused fixed animals were post-fixed in 4% potassium dichromate (pH 6.0) at 4°C for 6 h [15], washed in 0.1 M phosphate buffer (pH 7.4) and placed in 2% osmium for 4 h at room temperature, prior to embedding in Epon. Chromaffin-positive (chromaffin+) varicosities (i.e. varicosities containing catecholamines) were identified by their content of some dense-cored small (50 nm in diameter) synaptic vesicles (fig. 2b). Our previous study indicated that the great majority of chromaffin-negative (chromaffin-) varicosities are likely to be the SP/CGRP population [5]. Grids of serial sections were stained only with lead citrate so as to avoid false-positive staining.

Series of 55–74 longitudinal sections (100 nm thick) were cut from the mid region of 3 vessels from each of 3 WKY rats and 3 SHR. The middle section of each series was viewed in the electron microscope, and 5 axon bundles containing both chromaffin+ and chromaffin- profiles were selected from the middle two thirds of the vessel for analysis.

Analysis of Innervation

Vessel Dimensions. Vessel diameter was measured between medio-adventitial borders. Adventitial thickness was measured from the medio-adventitial border to the outer edge of the adventitia at the junction with the mesentery. The diameter of smooth muscle cells was derived from the medial thickness divided by the number of layers of smooth muscle.

Definitions

Varicosity and intervaricosity axon profiles, synaptic vesicles and neuromuscular junctions were defined as described previously [16]. 'Axons' includes all axon profiles, i.e. both varicosities and intervaricosities, whereas 'non-contacting varicosities' are varicosities found not to form a neuromuscular junction when traced in serial sections through their entirety [17].

Density of Sympathetic and Primary Afferent Innervation

Sections were analysed either directly in the microscope or from electron micrographs (enlarged to $\times 14,000$). The dimensions of the neural components were measured on approximately 180 μm^2 of vessel surface in individual sections of each vessel. Data for each animal were pooled.

The numbers of varicosity and intervaricosity profiles and the numbers of each that were SP+/SP- or chromaffin+/chromaffin- were determined along with their location in the adventitia. In addition, varicosities that formed neuromuscular junctions were counted. The density of axon bundles, axons, varicosities and neuromuscular junctions was calculated for each vessel and expressed per mm^2 vessel surface (i.e. medio-adventitial border [18]). As the sections were 0.1 μm thick, this value reflects the

density of each structure provided the dimensions of the structures being compared are the same [19]. This was confirmed directly here by serial reconstruction of varicosities of each type (table 3).

Distribution of Axon Bundles and Varicosities. The minimum distance of axon bundles and varicosities from the nearest smooth muscle cell was determined for all the axon bundles within the adventitia in sections of 3 SP-immunostained vessels (one from each of 3 animals of each strain). Distances were measured from electron micrographs ($\times 14,000$), using either a ruler and a $\times 1.5$ magnifying glass for non-contacting varicosities, or a micrometre graticule in a $\times 10$ magnifying lens for varicosities forming junctions. In addition, the number of varicosities that were bare of Schwann cells along their surface facing the smooth muscle was determined for SP+/- varicosities.

Dimensions of Chromaffin+ and Chromaffin- Varicosities and Neuromuscular Relationships. Sets of serial electron micrographs ($\times 14,000$) of 15 clearly chromaffin+ and 15 clearly chromaffin- varicosities were obtained from evenly spaced sites along vessels from 3 WKY rats and 3 SHR (i.e. 5 varicosities from each animal) and three-dimensional reconstructions were made [16]. None of these varicosities made neuromuscular junctions. Therefore, in addition, sections were scanned specifically to identify neuromuscular junctions; 5 junctions from WKY rats and 7 junctions from SHR rats were photographed in successive sections through the entire junction in a similar way. The following data were obtained using a graphics tablet and custom software [16]; varicosity and mitochondrial volume, number of small synaptic and large dense-cored vesicles and, in the case of the varicosities forming neuromuscular junctions, the area of neuromuscular contact.

Statistics

Data are presented as means \pm SEM throughout. Student's t test was used to determine whether there was a difference between vessels from SHR and WKY rats in the relationships between various innervation parameters. Significant differences were assumed when $p \leq 0.05$.

Results

Gross Structure of Second-Order Mesenteric Arteries

Vessel diameter, medial thickness and the number of layers of smooth muscle cells of second-order branches of mesenteric arteries from 7-week-old SHR were significantly larger than those from WKY rats. Although lumen diameter at maximal dilation was similar between the strains (fig. 1, table 1), the adventitia was significantly thinner in SHR than in vessels from WKY rats [12]. Because the derived diameter of smooth muscle cells ($\sim 4 \mu\text{m}$) was similar between strains, the hypertrophy of the media of arteries from SHR resulted from hyperplasia of the smooth muscle cells, in agreement with a previous report [3].

Table 1. Comparison of dimensions of second-order branches of mesenteric arteries from SHR and WKY rats (mean \pm SEM)

Rat strain	Outer diameter, μm	Inner diameter, μm	Media thickness, μm	Layers of smooth muscle cells	Adventitial thickness, μm
WKY	218 \pm 10	167 \pm 11	14 \pm 0.3	3.6 \pm 0.2	11.2 \pm 0.9
SHR	259 \pm 11	203 \pm 11	18 \pm 1	4.5 \pm 0.2	8 \pm 0.7
p value	0.01	0.34	0.005	0.001	0.01

Vessels were fixed at identical perfusion flow rates (1 ml/100 g body weight/h) after maximum dilatation. These measurements were obtained from 10 second-order branches of the mesenteric artery in each group.

Table 2. Densities of the components of the innervation around mesenteric arteries from SHR and WKY rats (means \pm SEM)

Rat strain	Axon bundles	Axons	SP- axons	SP+ axons	Total varicosities	SP- varicosities	SP+ varicosities	Junctions	Non-contacting varicosities
WKY (n = 6)	556 \pm 26	2,968 \pm 267	2,652 \pm 244	316 \pm 40	1,441 \pm 99	1,232 \pm 114	223 \pm 34	10 \pm 3	1,431 \pm 100 (n=5)
SHR (n = 5)	669 \pm 41	4,390 \pm 412	4,071 \pm 386	320 \pm 53	1,815 \pm 117	1,585 \pm 112	230 \pm 11	25 \pm 5	1,789 \pm 117
p value	0.03	0.01	0.01	0.95	0.03	0.05	0.83	0.03	0.04

Density values are all expressed per $10^3/\text{mm}^2$ of the outer surface of the media. n = Number of animals.

Distribution of VIP-Immunoreactive Axons

In comparison with the dense plexus of axons containing TH, VIP-immunoreactive axons were extremely rare around second-order mesenteric arteries from both SHR and WKY rats. They lay mainly as isolated axons branching in the outer adventitia distinct from the dense TH+ plexus that abuts the medio-adventitial border. The distribution of SP+ axons in this plexus has been described previously [5]. Structurally, the VIP+ axons were distinct from TH+ and SP+ axons in that VIP+ axons were very fine and had small varicosities. No differences could be detected between the number or distribution of VIP+ axons between vessels from SHR and WKY rats. The likelihood that the presence of these axons could lead to significant errors in this quantitative ultrastructural study seems very low and they have not been considered further here.

Quantitative Analysis of Perivascular Innervation

Innervation Density. As shown previously [3], the density of the innervation was greater in SHR than in WKY vessels (table 2). The density of axon bundles was 20% higher and that of axon profiles 48% higher around arteries from SHR. This reflected the greater numbers of SP- axons, which were approximately 53% more numerous

around SHR compared to WKY arteries. The density of SP+ axons was much lower and was identical between the two strains (table 2). The proportion of all axons that were SP+ was significantly ($p = 0.03$) lower in arteries from SHR ($7.3 \pm 1\%$, $n = 5$) than in WKY rats ($10.9 \pm 1\%$, $n = 6$). Thus the hyperinnervation involved only the noradrenergic population.

The proportion of axon profiles that were classified as varicosities was similar in vessels from WKY rats ($48 \pm 3\%$, $n = 3$) and SHR ($41 \pm 5\%$, $n = 3$, $p = 0.20$), but the density of varicosity profiles was $\sim 25\%$ higher around SHR than WKY rat vessels (table 2). This was again due entirely to higher numbers of SP- varicosity profiles, the density of SP+ varicosity profiles being similar between the strains (table 2).

The majority of varicosities were bare of Schwann cell towards the vessel surface, the proportion being similar between the two strains (WKY: $89 \pm 5\%$, $n = 3$; SHR: $81 \pm 3\%$, $n = 3$, $p = 0.17$). The proportion of SP+ varicosities that was bare was lower than for SP- ones but also did not differ between the strains (WKY: $61 \pm 12\%$; SHR: $66 \pm 6\%$, $p = 0.63$). However, the density of bare SP- varicosities was significantly greater in SHR vessels (WKY: $634 \pm 137 \times 10^3$ per μm^2 , $n = 3$; SHR: $1,240 \pm 58 \times 10^3$ per μm^2 , $n = 3$, $p = 0.007$).

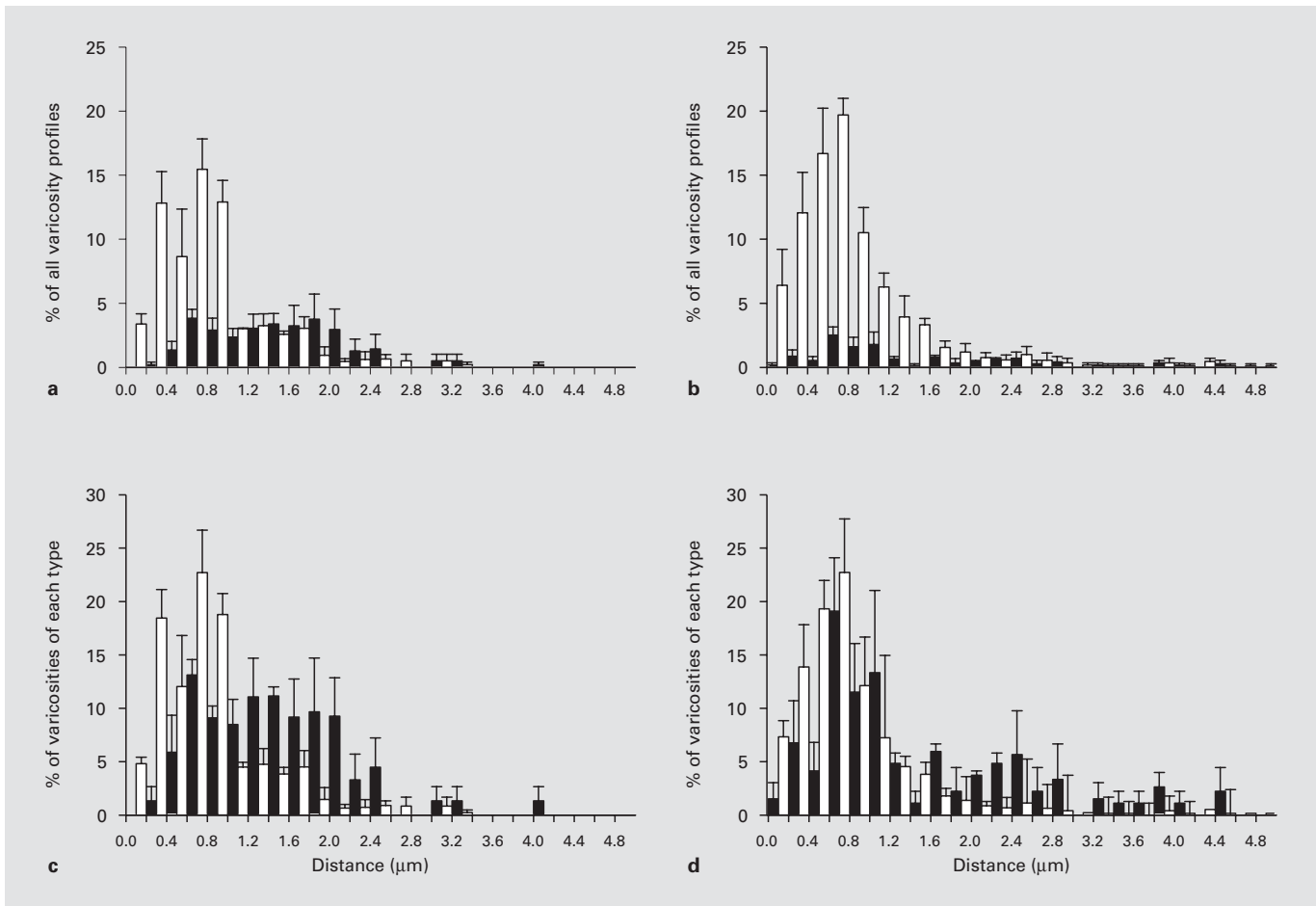


Fig. 3. Comparison of the distributions of SP+ (black columns) and SP- (white columns) varicosities around mesenteric arteries from WKY rats (**a, c**) and SHR (**b, d**). **a, b** Distributions of SP+ and SP- varicosities within the adventitia as a proportion of all varicosities. **c, d** Distributions of SP+ and SP- varicosities within the adventitia as a percentage of each varicosity type (data obtained from 3 vessels from 3 rats of each strain).

Distribution of the Innervation within the Adventitia

Axon bundles lay in the adventitia amongst collagen fibrils and fibroblasts in both strains. There were more axon bundles in the outer adventitia (>2 μm from the media) in SHR vessels than in those from WKY rats. However, the great majority of axon bundles lay within 1 μm of the medio-adventitial border in both strains (WKY: 79 ± 5%, n = 3, SHR: 85 ± 4%, n = 3, p > 0.05).

The mean number of axons per bundle was similar (WKY = 5.4 ± 0.4, n = 6; SHR = 6.5 ± 0.4, n = 5, p = 0.06), with the majority of bundles (WKY: 72 ± 8%; SHR: 62 ± 7%, p = 0.47) containing <5 axons. The proportion of large bundles was relatively small; however, only ~2% of bundles in WKY rat vessels but 15% of bun-

dles in SHR vessels contained >15 axons. These large bundles lay close (<1 μm) to the smooth muscle. These data suggest that extensive branching of axons occurs as the axons approach within 1 μm of the muscle, particularly in vessels from SHR.

The proportion of axon profiles in each bundle that were classified as varicosities (about 35%) was similar throughout the media. When varicosities were present, the number per bundle ranged from 1 to 15 (mean WKY: 2.1 ± 0.1; SHR: 1.9 ± 0.4; p = 0.60). The majority of varicosities were located in bundles of all sizes <1 μm from the smooth muscle in both groups of vessels (WKY: 61 ± 7%, SHR: 72 ± 8%, p = 0.38). In both strains, 20–25% of bundles did not contain any varicosity profiles.

Table 3. Quantitative morphological characteristics of contacting and non-contacting varicosities innervating WKY and SHR mesenteric arteries

Rat strain	Varicosity			Mitochondrial			Density of SSV/ μm^3	LGV/ varicosity	Contact area, μm^2
	volume μm^3	SA μm^2	SA/volume	volume μm^3	SA μm^2	SA/volume			
<i>WKY (n = 3 rats)</i>									
Chromaffin+									
Non-contacting varicosities (n = 15)	0.67 ± 0.09	3.59 ± 0.37	5.76 ± 0.30	0.07 ± 0.01	1.16 ± 0.19	18.1 ± 0.8	679 ± 30	5 ± 1	–
Contacting varicosities (n = 5)	0.69 ± 0.30	3.84 ± 1.08	7.04 ± 1.27	0.07 ± 0.03	1.02 ± 0.43	18.1 ± 2.5	655 ± 73	10 ± 5	0.37 ± 0.16
Chromaffin–									
Non-contacting varicosities (n = 15)	0.53 ± 0.05	3.04 ± 0.18	5.92 ± 0.25	0.06 ± 0.01	0.91 ± 0.15	17.00 ± 1.0	721 ± 43	11 ± 1	–
<i>SHR (n = 3 rats)</i>									
Chromaffin+									
Non-contacting varicosities (n = 15)	0.62 ± 0.06	3.75 ± 0.27	6.42 ± 0.33	0.05 ± 0.01	0.88 ± 0.13	18.8 ± 1.4	722 ± 50	3 ± 0.7	–
p value	0.64	0.72	0.13	0.34	0.22	0.63	0.45	0.13	–
Contacting varicosities (n = 7)	0.71 ± 0.13	3.79 ± 0.45	5.79 ± 0.52	0.06 ± 0.02	1.02 ± 0.26	17.4 ± 1.3	703 ± 55	5 ± 0.8	0.28 ± 0.07
p value	0.95	0.97	0.28	0.97	0.99	0.77	0.57	0.21	0.53
Chromaffin–									
Non-contacting varicosities (n = 15)	0.67 ± 0.10	4.01 ± 0.38	6.64 ± 0.44	0.06 ± 0.01	0.95 ± 0.19	18.0 ± 1.0	622 ± 52	12 ± 2	–
p value	0.21	0.02*	0.15	0.94	0.85	0.45	0.14	0.74	–

SA = Surface area.; SSV = small synaptic vesicles; LGV = large granular vesicles. In each case, p refers to the difference between SHR and WKY animals. * p ≤ 0.5.

Distribution of SP+ Axons. In material stained for SP, 37% of all axon bundles contained SP+ axons. The percentage of SP ± axons per bundle was highest between 1 and 2 μm from the smooth muscle in both rat strains. Close (<1 μm) to the smooth muscle, the proportion of SP+ per bundle was small and did not differ significantly between the strains (WKY: 6 ± 0.3%; SHR: 11 ± 2%; p = 0.08).

The vast majority of varicosities were SP– (fig. 3a, b). SP+ varicosities were rarely present in bundles that came close (<400 nm) to the medio-adventitial border although this occurred slightly more often in the SHR group (fig. 3). In arteries from WKY rats, the great majority of SP+ varicosities (81 ± 3%) were evenly distributed between 0.6 and 2.2 μm from the smooth muscle [5], whereas in SHR the spatial distribution was different with the majority of SP+ varicosities (59 ± 12%) lying closer than 1.2 μm from the muscle (fig. 3c, d). The proportion of all varicosities that was SP+ was similar in the two strains (WKY: 16 ± 3%, n = 6; SHR: 13 ± 1%, n = 5, p = 0.32; fig. 3a, b; table 2).

Neuromuscular Junctions

The proportion of varicosity profiles that formed typical neuromuscular junctions [16] was significantly lower in vessels from WKY rats compared to SHR (WKY: 0.6

± 0.3%, n = 6; SHR: 1.4 ± 0.3%, n = 5, p = 0.05). Consequently, the density of junctions on SHR arteries was more than twice as high as in equivalent samples of arteries from WKY rats (table 2). In immunostained material, all neuromuscular junctions were SP– in both strains. In contrast, the density of non-contacting varicosities was only about 25% greater around vessels from SHR compared to WKY rats (table 2).

From each strain, 15 chromaffin+ and 15 chromaffin– non-contacting varicosities [17] were identified. As the frequency of neuromuscular junctions was very low, considerable amounts of additional tissue were searched to locate 5 contacting chromaffin+ varicosities from arteries of WKY rats and 7 from SHR for reconstruction. During these searches, no contacting chromaffin– varicosities were detected.

The neuromuscular junctions formed by chromaffin+ varicosities had contact areas of about 0.3 μm^2 in each strain (table 3), representing 8.5 ± 2.0% (WKY) and 8.6 ± 3.6% (SHR) of the total varicosity surface area. Neuromuscular contact area was correlated with varicosity size (fig. 4f) as in other vessels [17].

Morphometric Analysis of Reconstructed Varicosities Chromaffin+ Varicosities. As for other noradrenergic varicosities [17], clusters of small synaptic vesicles and a

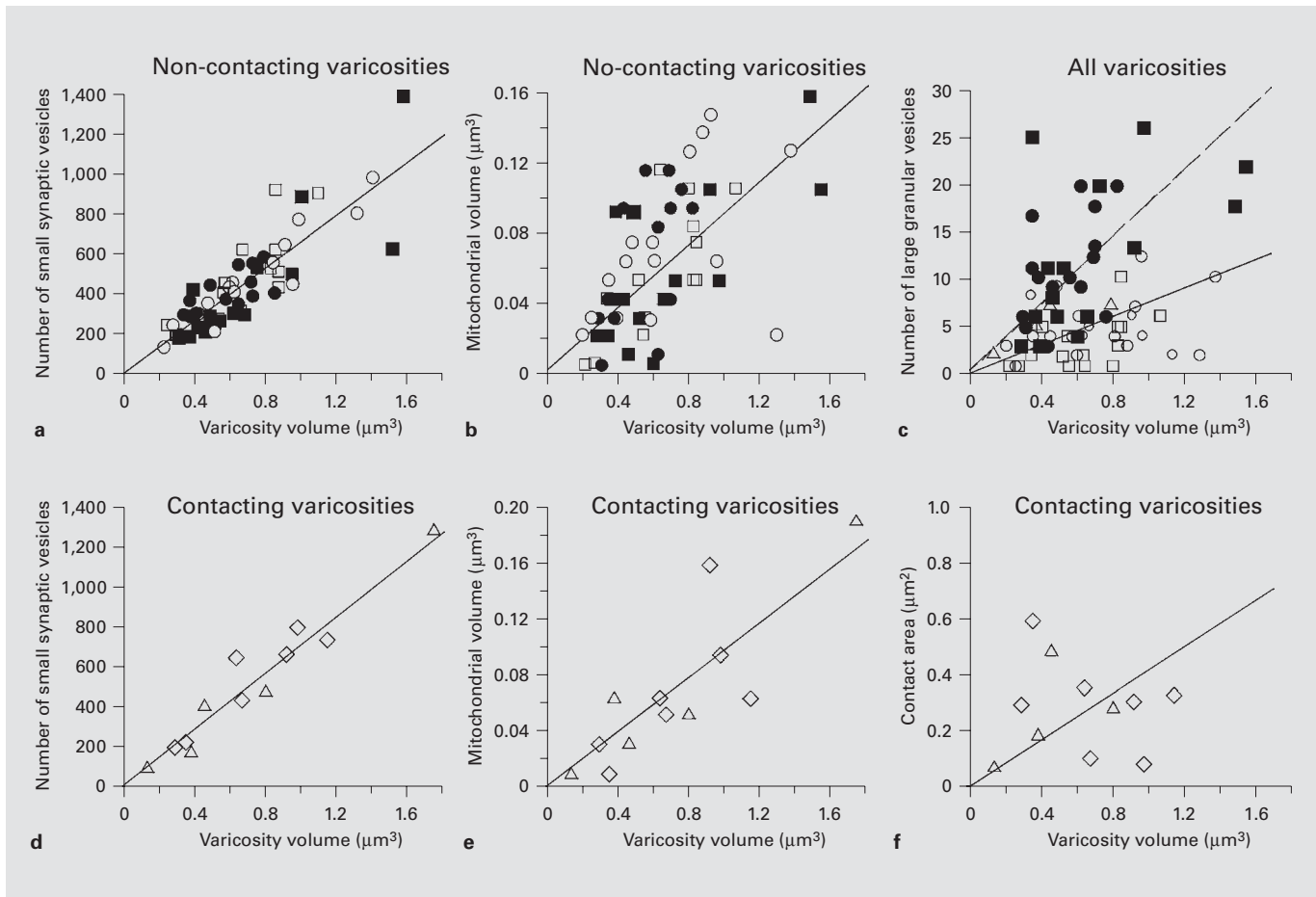


Fig. 4. Relation of morphological parameters to varicosity volume in reconstructed varicosities. Symbols show data for non-contacting varicosities (**a, b**) and all varicosities (**c**) in WKY rats (circles) and SHR (squares) and contacting varicosities (**d-f**) in WKY (triangles) and SHR (diamonds) rats. Noradrenergic (sympathetic) and SP+ (afferent) varicosities are shown by open and closed symbols, respectively. **a, d** Linear relation of the number of small synaptic vesicles to varicosity volume [$p < 0.0001$; slope = 674 (**a**), 700

(**d**); $r^2 = 0.94$ (**a**), 0.98 (**d**)]. **b, e** Linear relation between mitochondrial volume and varicosity volume [$p < 0.0001$; slope = 0.09 (**b**), 0.10 (**e**); $r^2 = 0.81$ (**b**), 0.89 (**e**)]. **c** Relation between the number of dense-cored vesicles and varicosity volume is steeper for SP+ (slope 17.5, $r^2 = 0.8$) than for SP- varicosities (slope 7.4, $r^2 = 0.70$). **f** Relation between neuromuscular contact area and varicosity volume in contacting varicosities ($p = 0.0002$, slope 0.41, $r^2 = 0.74$). Data obtained from 3 vessels from 3 rats of each strain.

few large dense-cored vesicles were present in all reconstructed chromaffin+ varicosities and each contained a single mitochondrion. The dimensions of these varicosities did not differ between the two strains of animals and there were also no differences in size between contacting and non-contacting varicosities in either strain (table 3). The size of the mitochondria, the numbers of small synaptic vesicles (about 400 per varicosity) and their density and the number of large granular vesicles (table 3) and relation of vesicles to varicosity size (fig. 4) did not differ whether or not the varicosities made contact or between the strains of rats (table 3).

Chromaffin-Negative Varicosities. This almost complete similarity in varicosity structure also applied to the varicosities that were chromaffin- (i.e. afferent), none of which contacted vascular smooth muscle cells (table 3, fig. 4). However, the varicosity surface area was 25% larger in the SHR than WKY strain (table 3); as varicosity volume was similar, this could have reflected a slight distortion of the varicosity shape. As recently reported [5], the number of large granular vesicles was higher in chromaffin- varicosities than in chromaffin+ ones ($p < 0.001$). This was the case in both rat strains, but the number was not strongly correlated with varicosity size (fig. 4c).

Discussion

The present study has demonstrated that the hyperinnervation of mesenteric arteries in SHR [2–4] is comprised of greater numbers of axon bundles, axons and varicosities than are present in these vessels in WKY rats. The quantitative data indicate that the hyperinnervation in SHR vessels is restricted to the chromaffin+/SP– (sympathetic) component of the perivascular plexus and includes more than twice the number of neurovascular junctions present in WKY vessels. Dimensionally, the sympathetic varicosities were virtually indistinguishable, and were almost identical to varicosities that contained SP, in both strains of rat. The differences in the innervation between the two strains, both with regard to the density of sympathetic axons and varicosities, and their distribution within the adventitia of the vessels are summarised semi-diagrammatically in figure 5.

The distribution of axons and varicosities was very similar between the strains, but in the SHR vessels there was evidence of greater branching and higher numbers of varicosities lying within 1 μm of the outer surface of the media of the artery. This applied to both sympathetic and SP+ varicosities, the latter lying closer to the vessel wall in tissue from SHR than WKY rats. The greater density of sympathetic varicosities in SHR arteries was detected despite the 15% greater diameter and surface area of the vessels, leading to the conclusion that the relative increase in the number of terminals per unit length of SHR vessel must be even larger than that estimated. On the same basis, the number of SP+ axons per unit length of vessel is probably slightly higher in SHR compared to WKY rats. It is possible that the higher numbers of axons/terminals in SHR arteries may also arise from a larger number of sympathetic neurons [20].

As in WKY rats [5], chromaffin+/SP– varicosities but not SP+ varicosities formed neuromuscular junctions. The greatest difference between the vessels from WKY and SHR rats was that the number of neuromuscular junctions identified in single sections was more than twice as high in the SHR vessels. This is a much larger difference than the 25% higher number of varicosities. As there were no dimensional differences between sympathetic varicosities or neuromuscular junctions of vessels from WKY rats and SHR (table 3) [19], the greater densities of profiles making junctions in single sections are likely to reflect real differences in the density of contacting varicosities. It is notable that there were no differences in the size of the junctions or areas of contact with the arterial smooth muscle and that the dimensions of junctions vary

substantially between vessels so far analysed [21]. The greater density of junctions in SHR vessels is consistent with electrophysiological data showing that the excitatory junction potentials evoked by perivascular nerve stimulation are larger in mesenteric arteries from SHR than WKY rats [22].

Neurally induced vasodilator responses of mesenteric arteries are similar for both SHR and WKY rats of similar age to those studied here (i.e. 8 weeks [23]), consistent with the similar density of the primary afferent terminals present in the two rat strains [24]. However, the vasodilatation becomes significantly smaller in vessels from older (15- and 30-week-old) SHR than age-matched WKY animals, in spite of a greater response to applied CGRP. This suggests that the density of the afferent innervation of mesenteric vessels in the SHR rats may decline with age [25].

Hyperinnervation of SHR vessels develops over the first 3–4 weeks of life before the development of hypertension. The hyperinnervation is associated with smooth muscle hyperplasia [3, 4] and is thought to follow the synthesis and release of greater amounts of NGF by the greater number of smooth muscle cells [26]. Smooth muscle cells of mesenteric arteries of SHR have five times normal levels of NGF mRNA at 10 days of age [26, 27], and tissue NGF levels are elevated above that in WKY vessels after 15 days of age [27, 28], when the perivascular plexus becomes established [29]. If NGF is supplied in excess by the smooth muscle in SHR arteries, the finding that the hyperinnervation is restricted to the sympathetic component of the perivascular plexus is surprising. Both sympathetic and sensory neurones are about 25% more numerous in SHR than in WKY rats [20], and their numbers are also increased when NGF levels are raised by increased target production [30]. These effects are due to a reduction in cell death during ontogeny. However, terminal sprouting of both sympathetic and primary afferent terminals would be expected if the concentration of NGF produced by the vascular smooth muscle cells is enhanced [30]. Such growth would, in any case, be necessary to achieve a normal density of primary afferent axons around the enlarged vessels. The selective excess of innervation by sympathetic axons implicates some factor additional to the raised levels of NGF in the SHR arteries.

One candidate is suggested by the raised concentrations of neurotrophin-3 (NT-3) present in sympathetic ganglia and the hyperinnervated target organs of SHR [31]. As afferent axons containing SP and CGRP are not modified in density or distribution in NT-3 knockout mice [32], it seems possible that the excess of this neurotrophin contributes to the selective sympathetic hypertrophy.

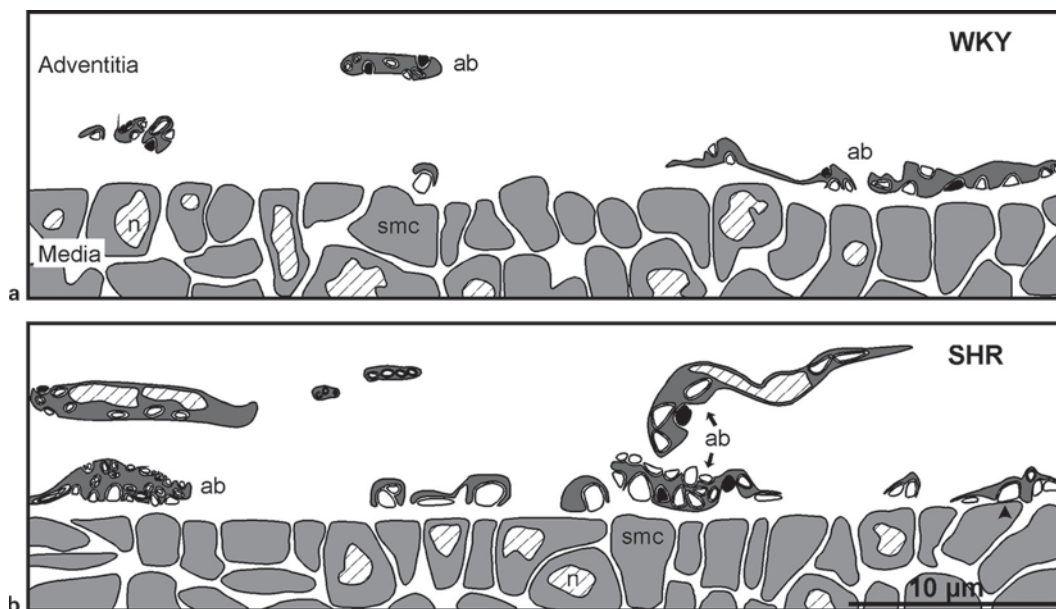


Fig. 5. Diagrammatic comparison of the innervation around vessels from SHR and WKY rats. Outlines were traced from low-power montages of electron micrographs of typical regions of vessels from WKY rats (**a**) and SHR (**b**). ab = Axon bundle; n = muscle cell nucleus; smc = smooth muscle cell. Arrowhead indicates varicosity forming a neuromuscular junction. Calibration applies to both parts of the figure. The greater number of axon bundles in SHR is clearly evident.

Alternatively, in SHR, sympathetic neurones may be more able than primary afferent neurones to respond to NGF, possibly because of a higher expression of neurotrophin receptors, either specific (e.g. *trkA*) or non-specific low-affinity neurotrophin receptors (p75NTR). While post-natal down-regulation of *trkA* occurs in some small sensory neurones independently of the levels of NGF, this is not the case for the SP+ population [33], which retains its dependence on NGF in the adult [34]. The p75NTR has been shown to be important for the normal development of sympathetic and primary afferent innervation of extracerebral vessels in mice [35]. Recent measurements show that mRNA for both *trkA* and p75NTR are elevated in neurones of the superior mesenteric ganglion of SHR rats at the age of the animals examined here [36]. Incidentally, the p75 receptor gene in SHR has been shown to have a point mutation that is linked to the expression of the hypertensive phenotype [37], and altered function of the p75NTR in SHR has been suggested to explain why the effects of excess NGF on sympathetic neurones are limited to axonal sprouting [36]. Further, raised NGF levels upregulate p75NTR in sympathetic neurones but not in dorsal root ganglion cells [38, 39], which would enhance the responsiveness of sympathetic neurones to both NGF

and NT-3. Thus vascular hyperinnervation in SHR may result as much from up-regulation of neurotrophin receptors on sympathetic terminals as from an excess of neurotrophins produced by the target tissue.

The vasodilator action of active perivascular afferents is thought to contribute to splanchnic hyperaemia during ischaemia and/or inflammation of the intestine [7]. Functionally, the lower density of afferent perivascular axons relative to noradrenergic ones in SHR might aggravate the hypertension by reducing any direct vasodilator effects of CGRP that counteract the noradrenergic constriction under those conditions. Such consequences have been demonstrated in mesenteric arteries from aged rats in which peptide levels are reduced [25].

In conclusion, this ultrastructural study has shown that the hyperinnervation of hypertrophied mesenteric arteries of SHR involves sympathetic but not primary afferent terminals in the perivascular plexus. There is marked enhancement of the density of neuromuscular junctions, paralleling the greater responses to nerve stimulation in these vessels [22]. The structural changes may result from a selective increase in responsiveness of sympathetic neurones to NGF and NT-3 due to the up-regulation of the p75NTR in perivascular terminals.

References

- Esler M, Jennings G, Lambert G, Meredith I, Horne M, Eisenhofer G: Overflow of catecholamine neurotransmitters to the circulation: source, fate, and functions. *Physiol Rev* 1990; 70:963–985.
- Head RJ: Hypertensive innervation: its relationship to functional and hyperplastic changes in the vasculature of the spontaneously hypertensive rat. *Blood Vessels* 1989;26:1–20.
- Lee RMKW: Vascular changes at the prehypertensive phase in the mesenteric arteries from spontaneously hypertensive rats. *Blood Vessels* 1985;22:105–126.
- Albert V, Campbell GR: Relationship between the sympathetic nervous system and vascular smooth muscle: a morphometric study of adult and juvenile spontaneously hypertensive rat/Wistar-Kyoto rat caudal artery. *Heart Vessels* 1990;5:129–139.
- Luff SE, Young SB, McLachlan EM: Ultrastructure of substance P-immunoreactive terminals and their relation to vascular smooth muscle cells of rat small mesenteric arteries. *J Comp Neurol* 2000;416:277–290.
- Li Y, Duckles SP: Effect of endothelium on the actions of sympathetic and sensory nerves in the perfused rat mesentery. *Eur J Pharmacol* 1992;210:23–30.
- Holzer P: Peptidergic sensory neurons in the control of vascular functions: mechanisms and significance in the cutaneous and splanchnic vascular beds. *Rev Physiol Biochem Pharmacol* 1992;121:49–146.
- Tsuda K, Masuyama Y: Effects of substance P on norepinephrine release from vascular adrenergic neurons in spontaneously hypertensive rats. *Am J Hypertens* 1991;4:327–378.
- Dunn WR, Hardy TA, Brock JA: Electrophysiological effects of activating the peptidergic primary afferent innervation of rat mesenteric arteries. *Br J Pharmacol* 2003;140:231–238.
- Rush RA, Chie E, Liu D, Tafreshi A, Zettler C, Zhou X-F: Neurotrophic factors are required by mature sympathetic neurons for survival, transmission and connectivity. *Clin Exp Pharmacol Physiol* 1997;24:549–555.
- Terenghi G: Peripheral nerve regeneration and neurotrophic factors. *J Anat* 1999;194:1–14.
- Lee RMKW, Triggler CR, Cheung DWT, Coughlin MD: Structural and functional consequence of neonatal sympathectomy on the blood vessels of spontaneously hypertensive rats. *Hypertension* 1987;10:328–338.
- Brock JA, van Helden DF, Dosen P, Rush RA: Prevention of high blood pressure by reducing sympathetic innervation in the spontaneously hypertensive rat. *J Auton Nerv Syst* 1996;61:97–102.
- Scott TM, Robinson J, Foote J: The peptidergic innervation of the developing mesenteric vascular bed in the rat. *J Anat* 1989;162:177–183.
- Ferguson M, Ryan GB, Bell C: Localization of sympathetic and sensory neurons innervating the rat kidney. *J Auton Nerv Syst* 1986;16:279–288.
- Luff SE, McLachlan EM, Hirst GDS: An ultrastructural analysis of the sympathetic neuromuscular junctions on arterioles of the submucosa of the guinea pig ileum. *J Comp Neurol* 1987;257:578–594.
- Luff SE, Young SB, McLachlan EM: Proportions and structure of contacting and non-contacting varicosities in the perivascular plexus of the rat tail artery. *J Comp Neurol* 1995;361:699–709.
- Luff SE, McLachlan EM: Frequency of neuromuscular junctions on arteries of different dimensions in the rabbit, guinea-pig and rat. *Blood Vessels* 1989;26:95–106.
- Luff SE, Hengstberger SG, McLachlan EM, Anderson WP: Distribution of sympathetic neuroeffector junctions in the juxtglomerular region of the rabbit kidney. *J Auton Nerv Syst* 1992;40:239–253.
- Messina A, Bertram J, Bakhle YS, Bell C: Decreased developmental cell death in sympathetic and spinal sensory nervous systems of the Kyoto spontaneously hypertensive rat. *J Hypertens* 1996;14:1111–1115.
- Luff SE: Ultrastructure of sympathetic axons and their structural relationship with vascular smooth muscle. *Anat Embryol* 1996;193:515–531.
- Brock JA, van Helden DF: Enhanced excitatory junction potentials in mesenteric arteries from spontaneously hypertensive rats. *Pflügers Arch* 1995;430:901–908.
- Kawasaki H, Saito A, Takasaki K: Age-related decrease of calcitonin gene-related peptide-containing vasodilator innervation in the mesenteric resistance vessel of the spontaneously hypertensive rat. *Circ Res* 1990;67:733–743.
- Kawamura K, Ando K, Takebayashi S: Perivascular innervation of the mesenteric artery in spontaneously hypertensive rats. *Hypertension* 1998;14:660–665.
- Li Y, Duckles SP: Effect of age on vascular content of calcitonin gene-related peptide and mesenteric vasodilator nerve activity in the rat. *Eur J Pharmacol* 1993;236:373–378.
- Head RJ: Hypertensive innervation and vascular smooth muscle hyperplastic change. *Blood Vessels* 1991;28:173–178.
- Falck PH, Harkin LA, Head RJ: Nerve growth factor mRNA content parallels altered sympathetic innervation in the spontaneously hypertensive rat. *Clin Exp Pharmacol Physiol* 1992;19:541–545.
- Zettler C, Rush RBR: Elevated concentrations of nerve growth factor in heart and mesenteric arteries of spontaneously hypertensive rats. *Brain Res* 1993;614:15–20.
- Luff SE: Development of neuromuscular junctions on small mesenteric arteries of the rat. *J Neurocytol* 1999;28:47–62.
- Davis BM, Fundin BT, Albers KM, Goodness TP, Cronk KM, Rice FL: Overexpression of nerve growth factor in skin causes preferential increases among innervation to specific sensory targets. *J Comp Neurol* 1997;387:489–506.
- Zhang SH, Rush R: Neurotrophin 3 is increased in the spontaneously hypertensive rat. *J Hypertens* 2001;19:2251–2256.
- Ernfors P, Lee KF, Kucera J, Jaenisch R: Lack of neurotrophin-3 leads to deficiencies in the peripheral nervous system and loss of limb proprioceptive afferents. *Cell* 1994;77:503–512.
- Bennett D, Averill S, Clary D, Priestley J, McMahon S: Postnatal changes in the expression of the trkA high-affinity NGF receptor in primary sensory neurons. *Eur J Neurosci* 1996;8:2204–2208.
- Molliver D, Snider W: Nerve growth factor receptor TrkA is down-regulated during postnatal development by a subset of dorsal root ganglion neurons. *J Comp Neurol* 1997;381:428–438.
- Kawaja MD: Sympathetic and sensory innervation of the extracerebral vasculature: roles for p75NTR neuronal expression and nerve growth factor. *J Neurosci Res* 1998;52:295–306.
- Krol KM, Kawaja M: Structural and neurochemical features of postganglionic sympathetic neurons in the superior mesenteric ganglion of spontaneously hypertensive rats. *J Comp Neurol* 2003;466:148–160.
- Nemoto K, Kageyama H, Ueyama T, Fukamachi K, Sekimoto M, Tomita I, Senba E, Forehand CJ, Hendley ED: Mutation of low affinity nerve growth factor receptor gene is associated with the hypertensive phenotype in spontaneously hypertensive inbred rat strains. *Neurosci Lett* 1996;210:69–72.
- Zhou X-F, Rush RJC: Endogenous nerve growth factor is required for regulation of the low affinity neurotrophin receptor (p75) in sympathetic but not sensory ganglia. *J Comp Neurol* 1996;372:37–48.
- Coome G, Kawaja M: Prolonged exposure to elevated levels of endogenous nerve growth factor affects the morphological and neurochemical features of sympathetic neurons of postnatal and adult mice. *Neuroscience* 1999; 90:941–955.